Thermal characterization and microstructure change of cobalt oxides

Chen-Bin Wang*, Hung-Kuan Lin, and Chih-Wei Tang

Department of Applied Chemistry, Chung Cheng Institute of Technology, National Defense University, Tahsi, Taoyuan, 33509 Taiwan, Republic of China

Received 11 November 2003; accepted 28 January 2004

A series of cobalt oxides with different oxidation states have been prepared by using a precipitation-oxidation method and a controlled reduction method (*in situ* thermogravimetry-temperature programmed reduction, STG-TPR). The gradual change in microstructure with different oxides is studied by transmission electron microscopy (TEM) and X-ray diffraction (XRD). The results show that high-valence cobalt oxide is hexagonal with an elongated shape, Co_3O_4 is spinel with hollow spheroidal shape and CoO is a face-centered cubic structure, respectively.

KEY WORDS: cobalt oxide; STG-TPR; thermal characterization; microstructure.

1. Introduction

The great interest in cobalt oxides is due to their high activity in the field of CO oxidation [1–5] and hydrocarbons oxidation [6–8]. Also, cobalt oxide is important in rechargeable batteries [9–11] and CO sensor [12–15] applications. Among cobalt oxides we know that Co_3O_4 and CoO are stable [16,17] and active for CO and hydrocarbons oxidation. While, the high-valence cobalt oxides are thermally unstable and not commercially available in chemistry market.

In previous experiments [4,5], in order to have better control in the preparation of high-valence cobalt oxides and obtain pure cobalt oxides to apply in the CO oxidation, we adapted the precipitation-oxidation method and temperature programmed reduction (TPR) technique. The CO oxidation activity decreased significantly with the oxidation state of cobalt, i.e., $CoO(+2) \gtrsim Co_3O_4(+8/3) \gg CoO(OH)\ (+3) \gtrsim CoO_x(> +3)$. Because the decomposition and reduction of CoO(OH) is fast and difficult to separate under temperature programmed decomposition (TPD) or TPR controlled. In this paper, we have chosen the *in situ* thermogravimetry-temperature programmed reduction (STG-TPR) method. The combination of the adjustment of heating rate with the weight loss of oxide species under STG-TPR, we easily prepare a series of pure cobalt oxide and understand the degree of reduction of cobalt oxides. For evaluating the microstructure changes, further, we have employed transmission electron microscopy (TEM), X-ray diffraction (XRD) and infrared spectroscopy (IR).

* To whom correspondence should be addressed.
E-mail: chenbin@ccit.edu.tw

2. Experimental

2.1. Sample preparation

The high-valence cobalt oxide (marked as CoO_x) was synthesized by the precipitation-oxidation method in an aqueous solution. The detailed preparation procedure was described in a previous paper [4]. Further, other pure cobalt oxide species were obtained by a controlled reduction method. The STG-TPR procedure was under the adequate heating rate (RS means that the slow heating rate is 0.25 °C/min) of hydrogen flow in a Setaram TG-DSC 111 calorimeter to separate oxide species. The sensitivity of weight determination was 0.5 μg. The STG-TPO procedure was initiated from RT to 1100 °C at a rate of 10 °C/min in a 100 mL/min flow of air.

2.2. Techniques of characterization

A flow of He (purity 99.999%) was used in the TPD experiments to purge away the oxygen desorbed from the oxidized samples upon heating from RT to 950 °C at a rate of 10 °C/min. The rate of oxygen desorption was monitored by the TCD in the downstream of the He flow.

Thermal decomposition of cobalt oxides was carried out in a Seiko TG/DTA 300 system. A sample size of ~10 mg was loaded in the sample pan of the calorimeter for characterization. The sample temperature was raised from RT to 1100 °C at a rate of 10 °C/min in a 100 mL/min flow of air.

The XRD analyses of the samples were carried out using a Siemens D5000 diffractometer. The patterns were run with a Ni-filtered $CuK_{\alpha 1}$ radiation ($\lambda = 1.5405$ Å).

Cobalt oxides microstructures were characterized with the TEM (Hitachi H600-3). The samples for the electron microscopy were prepared by making an

1011-372X/04/0400–0069/0

ethanol suspension and deposed onto an undercoat of a holey carbon film.

3. Results and discussion

3.1. Characterizations of fresh sample – CoO_x

Figure 1 indicates the TPD spectrum obtained from CoO_x. The desorption of oxygen is shown in the TPD spectra by three peaks at different temperatures (T_d). They are designated as D_1 ($T_d = 270\,^\circ C$), D_2 ($T_d = 310\,^\circ C$) and D_3 ($T_d = 870\,^\circ C$), respectively. These peaks indicate that the decomposition of oxygen on CoO_x occurs in three consecutive steps. We assume that the prepared fresh sample of, CoO_x, probably contained a little amount of high oxidative state CoO_2. The following three successive steps occur when raising the temperature in the TPD system.

$$4CoO_2 \cdot H_2O \rightarrow 4CoO(OH) + O_2 + 2H_2O \quad (1)$$

$$12CoO(OH) \rightarrow 4Co_3O_4 + O_2 + 6H_2O \quad (2)$$

$$2Co_3O_4 \rightarrow 6CoO + O_2. \quad (3)$$

The relative areas of D_1, D_2 and D_3 are 0.10, 0.97 and 2.80, respectively. Comparison of these areas with the theoretical values (3, 1 and 2, respectively) based on the equations 1 to 3, indicates that CoO_x consists of mainly CoO(OH) and a little amount of CoO_2.

Figure 2 shows the TG/DTG curves for the decomposition of CoO_x in a dynamic nitrogen (100 ml/min) flow. The TG curve shows three weight loss steps and the DTG curve shows the maximum loss rate at 280, 325 and 890 °C (labeled as G_1, G_2 and G_3), respectively. Prior to 280 °C, the tardy weight loss should be the desorption of water on CoO_x surface in a heating process. Weight loss of 3.6% in step G_1 is mainly the decomposition of CoO_2 into CoO(OH) according to equation (1) (theoretical weight loss is 16%). Obviously,

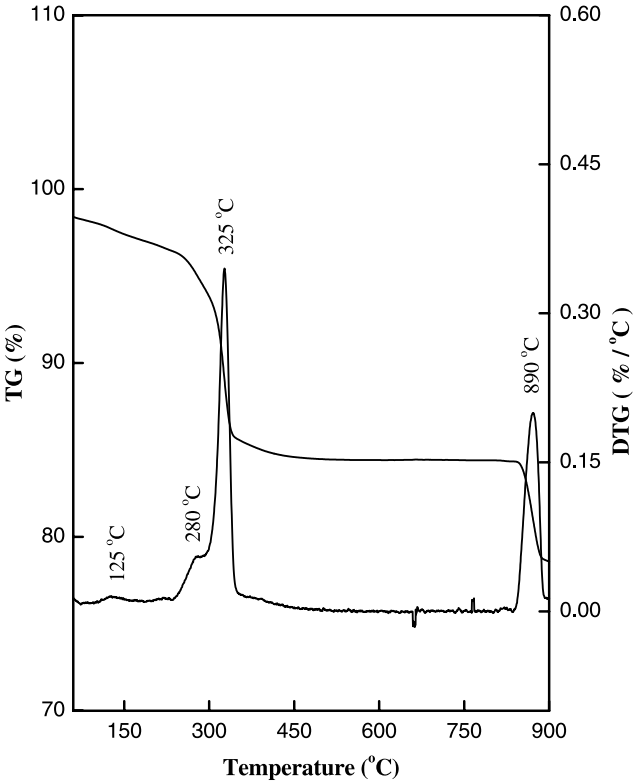

Figure 2. The TG (top curve) and TDG profiles of CoO_x.

only a little amount of CoO_2 exists. Weight loss of 10.5% in step G_2 should be decomposed of CoO(OH) into Co_3O_4 according to equation (2) (theoretical weight loss is 12.7%). Weight loss of 6.4% in step G_3 is the decomposition of Co_3O_4 into CoO according to equation (3) that is close to the theoretical value (6.6%). Therefore, CoO_x is suggested that contains CoO(OH), CoO_2, and surface water.

According to the above results and the previous study [5], we find that the phase transformation between CoO(OH) and Co_3O_4 is fast and difficult to separate using either the TPD, TPR or TG system. Furthermore,

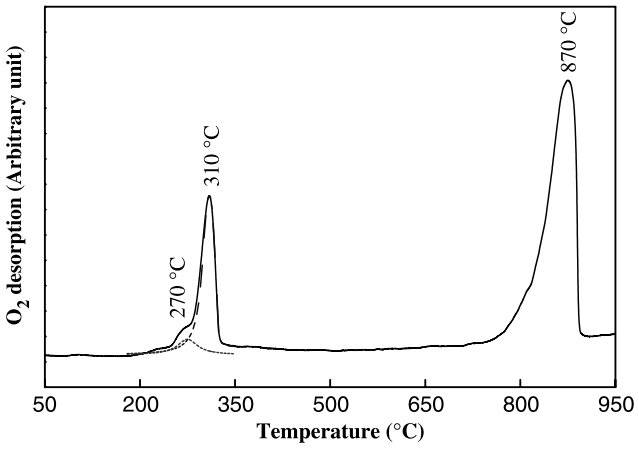

Figure 1. The TPD spectrum of CoO_x.

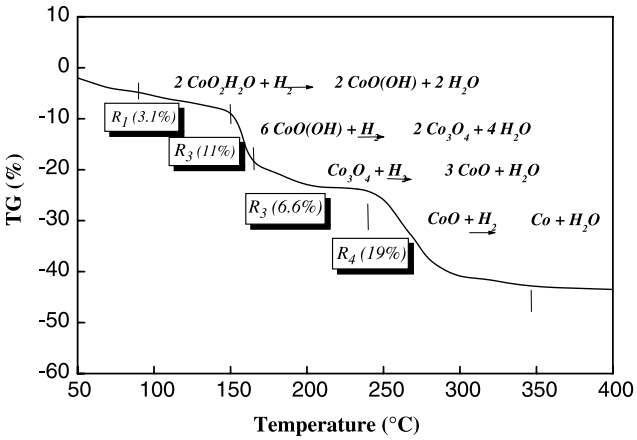

Figure 3. The STG-TPR profile of CoO_x in a dynamic hydrogen environment.

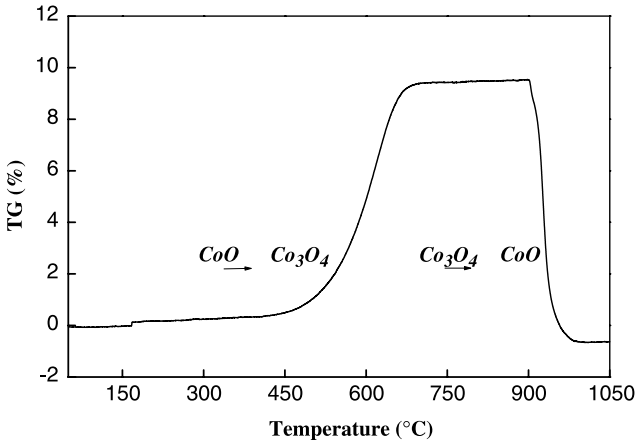

Figure 4. The STG-TPO profile of CoO in a dynamic air environment.

we chose the STG-TPR method in a dynamic hydrogen (100 mL/min) flow. Figure 3 shows the STG-TPR profile of CoO_x and possible reductive reactions. The curve shows four main regions of weight loss (labeled as R_1, R_2, R_3 and R_4) of CoO_x in the range of 90–140, 140–160, 160–230 and 230–380 °C, respectively. Prior to 90 °C, the tardy weight loss should be the desorption of water on CoO_x surface in hydrogen environment. A comparison of the STG-TPR trace with TG/DTG (figure 2) reveals that consecutive steps can be assigned to the reduction of CoO_2, CoO(OH), Co_3O_4 and CoO species in R_1, R_2, R_3 and R_4 region, respectively. Accordingly, the following four successive steps are designated in STG-TPR on raising the sample temperature.

$$2CoO_2 \cdot H_2O + H_2 \rightarrow 2CoO(OH) + 2H_2O \quad (4)$$

$$6CoO(OH) + H_2 \rightarrow 2Co_3O_4 + 4H_2O \quad (5)$$

$$Co_3O_2 + H_2 \rightarrow 3CoO + H_2O \quad (6)$$

$$CoO + H_2 \rightarrow Co + H_2O. \quad (7)$$

Weight loss of 3.1% in region R_1 is mainly the reduction of CoO_2 into CoO(OH) according to equation (4) (theoretical weight loss is 16%). This is the same as the TG/DTG result in step G_1, where only a little amount of CoO_2 exists. A weight loss of 11% in region R_2 should be reduced of CoO(OH) into Co_3O_4 according to equation (5) (theoretical weight loss is 12.7%). Weight loss of 6.6% in region R_3 is the reduction of Co_3O_4 into CoO according to equation (6); that is same as the theoretical value. Weight loss of 19.5% in region R_4 should be reduced of CoO into Co metal according to equation (7) (theoretical weight loss is 21.3%).

For clarification of the reduction extent of cobalt oxide for the reduced sample, we performed the temperature-programmed oxidation (TPO) studies of the region R_3 specimen (CoO). STG-TPO profile of the re-oxidation of the species, CoO, is shown in figure 4. The re-oxidation is performed in a dynamic air (100 ml/min) flow. Observed changes in a sample weight indicated that CoO (a p-type oxide) is oxidized by air to Co_3O_4 while raising the temperature over 500 °C and that the formed Co_3O_4 (a n-type oxide) is subsequently decomposed back to CoO at 1000 °C:

$$6CoO + O_2 \Leftrightarrow 2Co_3O_4 \quad (8)$$

Obviously, CoO and Co_3O_4 are stoichiometric oxides of cobalt that are stable in air at low temperatures. Co_3O_4 is preferred at 500 °C < T < 1000 °C while CoO dominates at T > 1000 °C.

3.2. Microstructures of cobalt oxide derivatives

In order to prepare pure cobalt oxides and cobalt metal, three oxide derivatives – CoO(OH), Co_3O_4, CoO and Co from CoO_x – are prepared in hydrogen environment under STG-TPR system. The sample temperature is controlled at a rate of 0.25 °C/min from room temperature to 130, 150, 220 and 350 °C [labeled as RS-130, RS-150, RS-220 and RS-350], respectively and stays at that temperature for 3 h before cooling down naturally in ambient temperature.

Figure 5 presents XRD patterns for cobalt oxide derivatives. The diffraction profiles of the CoO_x and RS-130 samples are almost identical. It indicates that the pattern matches the JCPDS 14-0673 file identifying cobalt oxyhydroxide, CoO(OH), with a hexagonal structure. From the XRD pattern, it is clear that CoO_x undergoes changes in its composition and structure under a hydrogen environment up to a temperature above 150 °C. The RS-150 sample converts into a cobaltic oxide with a spinel structure [Co_3O_4], the RS-220 sample turns into a cobaltous oxide with a face-centered cubic (fcc) structure [CoO] and the RS-350 was reduced to cobalt metal with a fcc structure [Co].

The microstructures of cobalt oxide derivatives and the systematic changes accompanying the onset of dehydration and reduction of CoO_x have been distinguished by comparative examination of the TEM.

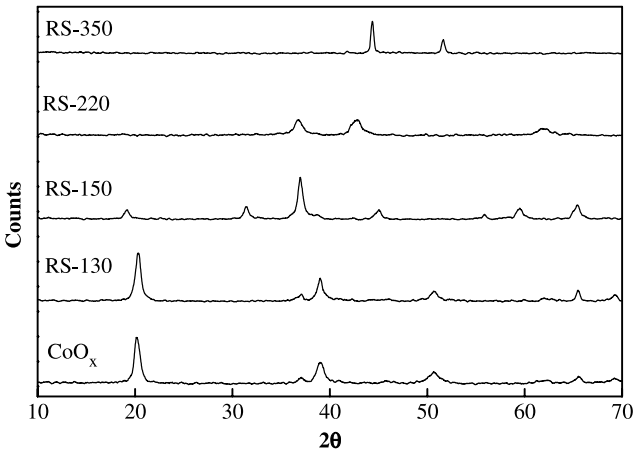

Figure 5. XRD characterization for a series of cobalt oxide derivatives.

Figures 6–11 present the TEM images of sample under STG-TPR treatment. Some important observations are shown below.

Figure 6 indicates that the CoO_x sample possesses an elongated shape with a random orientation which is covered by the thickness of an amorphous phase. On comparing with the TEM results of figures 6 and 7, the RS-130 sample [CoO(OH)] also presents the distinct elongated shape with a random orientation (figure 7) while the covered amorphous phase has been removed under the dehydration and reduction processes. Both samples possess the identical hexagonal structure and have been identified from the XRD pattern. TEM studies further confirmed that the microstructure remained unchanged.

As the reductive temperature reaches 150 °C, a marked change in the morphology is evident for the RS-150 sample [Co_3O_4]. The most significant feature is the formation of overlayers of a hollow spheroidal shape (figure 8). The Co_3O_4 crystallites of a hollow spheroidal shape (the hollow inside diameter is 80–180 nm) are the main Co-containing phases. They are similar to the particles observed earlier by Potoczna-Petru *et al.* in [18] and described as the torus shaped ones. No hollow spheroidal particles can be detected when the temperature raises to 220 °C (RS-220 sample, [CoO]). The partially facetted CoO formed (figure 9) after the reduction of Co_3O_4.

Figure 7. TEM micrograph for the RS-130 sample [CoO(OH)].

Figure 6. TEM micrograph for the CoO_x.

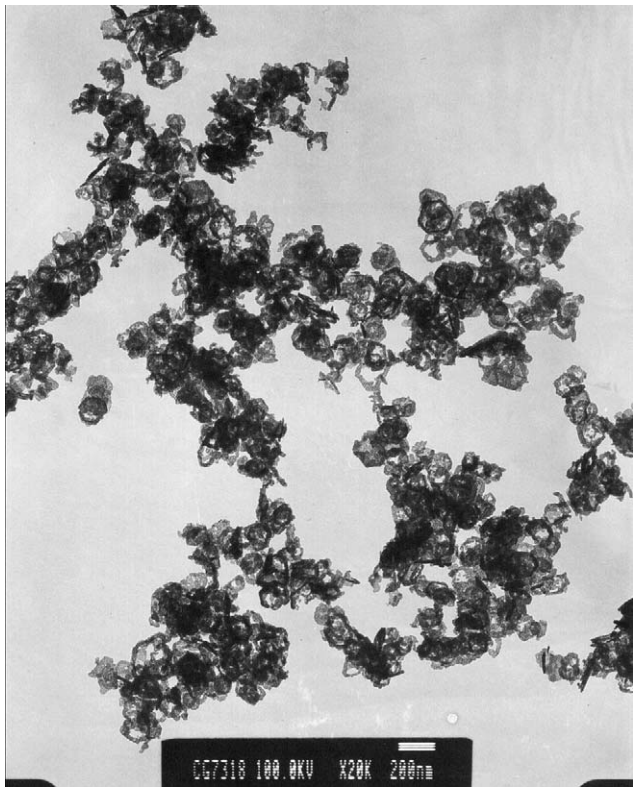

Figure 8. TEM micrograph for the RS-150 sample [Co_3O_4].

Figure 9. TEM micrograph for the RS-220 sample [CoO].

Figure 10. TEM micrograph for the RS-220 sample heating to 800 °C under air environment [Co_3O_4].

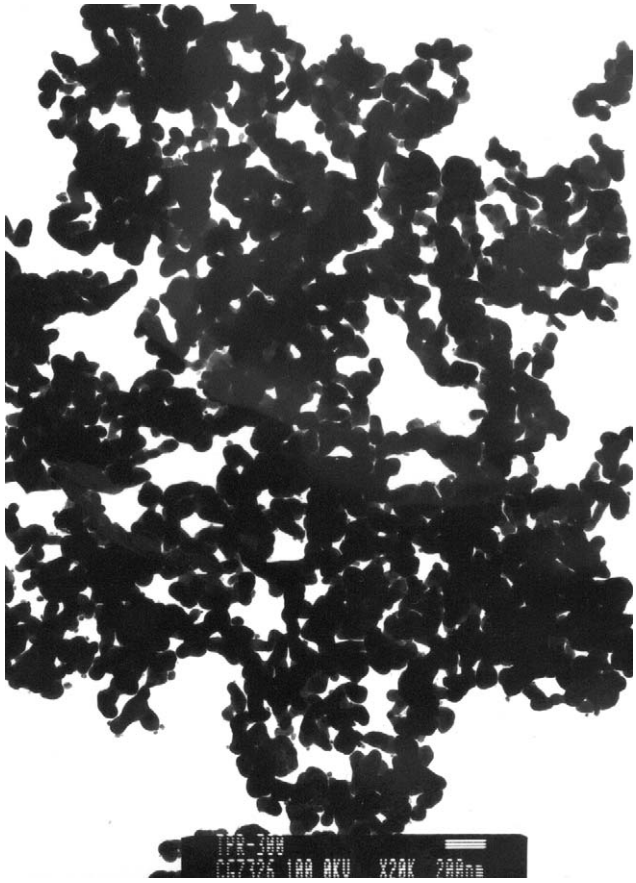

Figure 11. TEM micrograph for the RS-350 sample [Co].

Influence of reduction-oxidation treatment on the microstructure of Co_3O_4 has also been investigated with TEM (figure 10). According to the STG-TPO result (figure 4), we know that the Co_3O_4 can be formed from CoO under air when the temperature is above 500 °C. We chose the RS-220 sample, heating to 800 °C under air atmosphere. The photograph indicates that the morphology of Co_3O_4 is unaltered after the reduction-oxidation process. The agglomeration of Co_3O_4 from the dispersed CoO species under oxidation is not observed. However, the coagulation of cobalt particles is enhanced (figure 11) when raising the reductive temperature to 350 °C (RS-350). Metallic cobalt particles obtained from thermal reduction of the CoO_x precursor show different morphological characteristics. The sample lost the elongated shape by sintering as a consequence of the heating process.

4. Conclusion

We have shown that a STG-TPR method based on the controlling of the heating rate with weight loss of oxide specimen to refine pure cobalt oxides and cobalt metal. The concentrated results are summarized in table 1. The following conclusions have been made:

Table 1
Characterization and microstructures of cobalt oxide derivatives

Sample	Composition	T_d/°C		XRD	TEM
		TPD	TG		
CoO_x	Mixed oxides (Little CoO_2)	–	–	Hexagonal	Elongated shape with a random orientation (covered by the thickness of an amorphous phase)
RS-130	CoO(OH)	270	280	Hexagonal	Distinct elongated particle with a random orientation
RS-150	Co_3O_4	310	325	Spinel	Ring of a hollow spheroidal shape formed (inside diameter is 80–180 nm)
RS-220	CoO	870	890	fcc	Partially facetted formed
RS-350	Co	–	–	fcc	Coagulation of cobalt particles

1. The decomposition of CoO_x using the TPD or TG method proceeded in three consecutive steps, i.e.,

$$CoO_x \xrightarrow{T_d\sim 270\text{–}280\,^\circ C} CoO(OH) \xrightarrow{T_d\sim 310\text{–}330\,^\circ C} Co_3O_4 \xrightarrow{T_d\sim 870\text{–}890\,^\circ C} CoO$$

2. The reduction of CoO_x in STG-TPR proceeded (under 0.25 °C/min heating rate) in four consecutive steps, i.e.,

$$CoO_x \xrightarrow{T_r\sim 130\,^\circ C} CoO(OH) \xrightarrow{T_r\sim 150\,^\circ C} Co_3O_4 \xrightarrow{T_r\sim 200\,^\circ C} CoO \xrightarrow{T_r\sim 350\,^\circ C} Co$$

3. High-valence cobalt oxide is hexagonal with an elongated shape, Co_3O_4 is spinel with a hollow spheroidal shape and CoO is a face-centered cubic structure.

Acknowledgment

The authors acknowledge the financial support for this study by the National Science Council of the Republic of China.

References

[1] P. Thormählen, M. Skoglundh, E. Fridell and B. Andersson, J. Catal. 188 (1999) 300.
[2] J. Jansson, J. Catal. 194 (2000) 55.
[3] J. Jansson, A.E.C. Palmqvist, E. Fridell, M. Skoglundh, L. Österlund, P. Thormählen and V. Langer, J. Catal. 211 (2002) 387.
[4] H.K. Lin, C.B. Wang, H.C. Chiu and S.H. Chien, Catal. Lett. 86 (2003) 63.
[5] H.K. Lin, H.C. Chiu, H.C. Tsai, S.H. Chien and C.B. Wang, Catal. Lett. 88 (2003) 169.
[6] E. Garbowski, M. Guenin, M.C. Marion and M. Primet, Appl. Catal. 64 (1990) 209.
[7] A.S.K. Sinha and V. Shankar, J. Chem. Eng. Biochem. Eng. 52 (1993) 115.
[8] K. Ivanov, Appl. Catal. A116 (1994) L1.
[9] F. Lichtenberg and K. Kleinsorgen, J. Power Sources 62 (1996) 207.
[10] E. Antolini and E. Zhecheva, Mater. Lett. 35 (1998) 380.
[11] T.J. Boyle, D. Ingersoll, T.M. Alam, C.J. Tafoya, M.A. Rodriguez, K. Vanheusden and D.H. Doughty, Chem. Mater. 10 (1998) 2770.
[12] K. Omata, T. Takada, S. Kasahara and M. Yamada, Appl. Catal. A146 (1996) 255.
[13] H. Yamaura, J. Tamaki, K. Moriya, N. Miura and N. Yamazoe, J. Electrochem. Soc. 144 (1997) L158.
[14] H. Yamaura, K. Moriya, N. Miura and N. Yamazoe, Sensors Actuators B65 (2000) 39.
[15] E. Gulari, C. Güldür, S. Srivannavit and S. Osuwan, Appl. Catal. A182 (1999) 147.
[16] D.R. Lide, *Handbook of Chemistry and Physics* 72nd ed. (1991–1992).
[17] R.B. King, *Encyclopedia of Inorganic Chemistry*, Vol. 2 (John Wiley and Sons, 1994)
[18] D. Potoczna-Petru, J.M. Jablonski, J. Okal and L. Krajczyk, Appl. Catal. A175 (1998) 113.